Agricultural and Forest Meteorology 237–238 (2017) 143–149

Contents lists available at ScienceDirect

Agricultural and Forest Meteorology

journal homepage: www.elsevier.com/locate/agrformet

Short communication

Influence of levelling technique on the retrieval of canopy structural parameters from digital hemispherical photography

Niall Origo[a,b,*], Kim Calders[a,b], Joanne Nightingale[a], Mathias Disney[b,c]

[a] Earth Observation, Climate and Optical group, National Physical Laboratory, Hampton Road, Teddington, Middlesex TW11 0LW, UK
[b] Department of Geography, University College London, Gower Street, WC1E 6BT, UK
[c] NERC National Centre for Earth Observation, UK

ARTICLE INFO

Article history:
Received 1 December 2016
Received in revised form 31 January 2017
Accepted 3 February 2017
Available online 16 February 2017

Keywords:
Plant area index
Sensor comparison
Levelling
Hemispherical photography

ABSTRACT

Digital hemispherical photography is a simple, non-destructive method for estimating canopy biophysical parameters for ecological applications and validation of remote sensing products. Determination of optimum and repeatable acquisition procedures is well documented in the literature but so far this has not focused on evaluating the levelling procedure used to align the camera. In this paper, the standard recommendation that tripod levelling is a necessity is tested by comparing it with a hand-levelled procedure. The results show that the average difference between the two procedures is <2% for effective plant area index and <1% for gap fraction at the VALERI plot scale, which generally falls within the variance. Users implementing the hand-levelled technique can expect large reductions in data acquisition time, allowing many more samples to be collected without compromising the overall quality of the data retrieved.

1. Introduction

The application of hemispherical photography to the characterisation of the radiative and structural properties of tree and crop canopies has been widely used since the 1960s (Chianucci and Cutini, 2012). The advent of digital cameras and hence digital hemispherical photography (hereafter referred to as DHP) has transformed the ease with which canopy measurements can be made and analysed. The cost of purchasing a DHP system is well within the range of most research budgets, which goes a long way to explain the technique's popularity. As a result, DHP has been used in a large number of application areas such as hydrology, carbon and global change (Sea et al., 2011; Chianucci and Cutini, 2012) to quantify canopy biophysical parameters such as leaf/plant area index (LAI/PAI) and photosynthetically active radiation (PAR) (Leblanc et al., 2005). Furthermore, DHP is often used to collect validation data for remote sensing based estimates of canopy biophysical products (Baret et al., 2003; Morisette et al., 2006; Sea et al., 2011).

The image derived from DHP can be seen as raw data: processing is required to return meaningful parameters related to the canopy. PAI estimates can be retrieved from DHP through quantifying gaps in the canopy at a particular point, and relating these to the overall canopy area to give canopy gap fraction or gap probability (P_0). The relationship between gap fraction and PAI depends on the assumptions that are made in quantifying gaps in a DHP, which in turn depends on the way the DHPs are analysed (e.g. clumping/non-clumping, all view zeniths/57.5°, etc.); whichever is utilised, inversion of the gap fraction model is the common procedure to retrieve PAI. It is worthwhile noting that since most DHP processing techniques do not remove the wood component from consideration, the derived variable is PAI rather than LAI (Woodgate et al., 2016). For this reason PAI is used here instead of LAI. This paper utilises the LAI and PAI definitions set out in Fernandes et al. (2014):

- **LAI**: half of the green leaf area per unit of horizontal ground surface area (Chen and Black, 1992).
- **PAI**: half of the surface area of all above ground vegetation matter per unit of horizontal ground surface area.

Despite its many advantages, it has been noted by a number of authors (Pueschel et al., 2012; Glatthorn and Beckschäfer, 2014; Macfarlane et al., 2014; Schaefer et al., 2014) that standardisation of the image acquisition and processing procedure is required in order to ensure that data is comparable between sites and users. For example, correct determination of exposure settings (Chianucci

* Corresponding author at: Earth Observation, Climate and Optical group, National Physical Laboratory, Hampton Road, Teddington, Middlesex, TW11 0LW, UK.
E-mail address: niall.origo@npl.co.uk (N. Origo).

http://dx.doi.org/10.1016/j.agrformet.2017.02.004

and Cutini, 2012; Glatthorn and Beckschäfer, 2014; Woodgate et al., 2015), choice of file format and image band choice (Pueschel et al., 2012), and thresholding algorithm and settings (Promis et al., 2011; Pueschel et al., 2012; Woodgate et al., 2015) have been shown to produce significant differences in the resulting gap fraction estimates. In situ protocols (Schaefer et al., 2014; AusCover, 2015; TERN, 2015) offer reasonable procedures to minimise these effects. However, without a 'truth' value (i.e. a measurement technique that can provide a benchmark) consistency between the different measurement techniques and/or configurations is seen as the next best alternative.

The current consensus between the majority of protocols and studies utilising DHP is the assertion that the camera must be levelled using a tripod (Chianucci and Cutini, 2012; AusCover, 2015; TERN, 2015; Woodgate et al., 2015). Levelling is an important component in ensuring that images taken within and between sites are comparable. It is based on two principles: (1) that the camera is orientated so that the line passing through image centre is perpendicular to the ground (i.e. pointing into the sky) and the same position in the image represents magnetic north, and (2) that the camera remains in the same position for the duration of the image acquisition. A tripod and bubble level are commonly used to accomplish this on both sloping and flat terrain, where the former utilises post-processing to correct for the effect of the slope (examples provided in España et al. (2008)). However levelling the camera can be the most time-consuming aspect of the sampling procedure. To our knowledge the effect of levelling accuracy on estimates of gap fraction and PAI remains unknown.

Here, hand-levelling is proposed as an alternative time-saving technique to tripod levelling for DHP image acquisition. In the absence of a suitable 'truth' P_0 or PAI the two levelling techniques are compared with respect to gap fraction at the image and subplot level as well as PAI at the subplot level. As far as we are aware, the results are the first quantitative comparison of hand-levelling with tripod-levelling during DHP collection in the field.

2. Materials and methods

The experiment took place in Wytham Woods, Oxford, UK, a temperate deciduous woodland, across a 6 ha subset of an established 18 ha Smithsonian plot (STRI, 2008). The 6 ha area is primarily composed of Sycamore (*Acer pseudoplatanus*), Ash (*Fraxinus excelsior*), and Hazel (*Corylus avellana*) (Butt et al., 2009). Within the 6 ha area of the Smithsonian plot, every 1 ha is subdivided into 25 subplots of 20 m^2 with flags placed within the subplot according to the VALERI sampling design (Baret et al., 2003). Tripod- and hand-levelled images were acquired at each point within the subplot. Fig. 1 shows the layout of the Smithsonian plot as well as the location of the subplots where the comparison data were collected. The subplots were chosen with the aim of sampling the natural variability and local scale topography within the 6 ha area.

2.1. Measurement setup

A Canon 5D (full-frame Digital Single-Lens Reflex) and Sigma 8 mm fisheye lens capable of acquiring images with a 180° field of view (FOV) were used in this study. The tripod-levelled images were acquired first since they took the longest to set up. The minimum possible time between data acquistion from the different techniques was desired to remove differences due to changing background and illumination conditions; generally the image pairs were acquired within 30 s of each other. The camera was set to record automatic exposure in high quality JPEG and RAW format.

Table 1
The threshold settings automatically selected by CAN-EYE; the same settings were used for the respective hand- and tripod-levelled image. Fig. 1 gives the locations of the subplots graphically.

Plot and subplot ID	Brightness[1]	Greenness[2]	Brownness[3]
P2S9	0.647	0.087	−0.181
P5S12	0.684	0.173	−0.246
P6S1	0.656	0.106	−0.174
P7S12	0.683	0.13	−0.142
P8S11	0.696	0.233	−0.311

* M. Weiss, pers. comm., (02.05.16).
1* Brightness = $\frac{R+G+B}{3}$.
2* Greenness = $3G - 2R - B$.
3* Brownness = $3B - 2R - G$.

2.1.1. Tripod levelling

The camera was placed on a tripod with the tip of the lens at 1.3 m above the ground (i.e. diameter at breast height; left and middle left of Fig. 2). A compass was used to orientate the bottom of the camera to north, while a triple-axis bubble level was used to ensure that the camera was level in the forward-backward (pitch) and left-right (roll) directions.

2.1.2. Hand levelling

The camera was held on a strap around the user's neck and raised to face-level such that the bottom of the lens was at eye-level. The bottom of the camera was away from the user and orientated north using the flags placed during the plot setup. The camera was aligned by eye using the bottom of the lens as the reference point. The images on the right of Fig. 2 show the procedure in practice.

2.2. Image processing

All images were processed using the CAN-EYE DHP processing software (INRA, 2013); CAN-EYE was chosen since it provides detailed outputs (e.g. within image gap fraction distribution, etc.) as well as providing the capability of producing both effective and clumping-corrected PAI (PAI_e and PAI respectively, where $PAI_e = \Omega PAI$ and Ω represents the clumping index). The RAW Canon image files were converted to JPEG before processing in CAN-EYE. Utilisation of the RAW Canon image file avoids the post-processing implemented by the camera in the from-camera JPEGs (Macfarlane et al., 2014). The lens projection function and image-lens centre offset values (acquired according to the CAN-EYE calibration procedure given in INRA (2013)) were provided as input to the software. Images were masked to 120° and a binary threshold applied according to the automatic settings provided by CAN-EYE (listed in Table 1). This was checked visually for a subsample of the images using a gamma adjustment ($\gamma = 2.2$).

CAN-EYE computes the gap fraction from the input images and inverts this to produce PAI based on all images from a VALERI plot. Importantly, estimating PAI from a single image is discouraged due to sampling considerations and because the clumping index (Ω) relies on multiple sample points for its calculation (Weiss et al., 2004). As a result CAN-EYE does not produce PAI based on a single image (INRA, 2013). For this reason, the image gap fraction (58 sample points) as well as the subplot aggregated values (PAI_e and gap fraction), for which there are 5 sample points, are used in the analysis to provide an adequate sample size. Details about the procedures used to calculate the aggregated parameters are described in INRA (2013). The results are discussed with reference to the root mean square error (RMSE), an estimate of the mismatch between the predicted relationship and the observed values; the

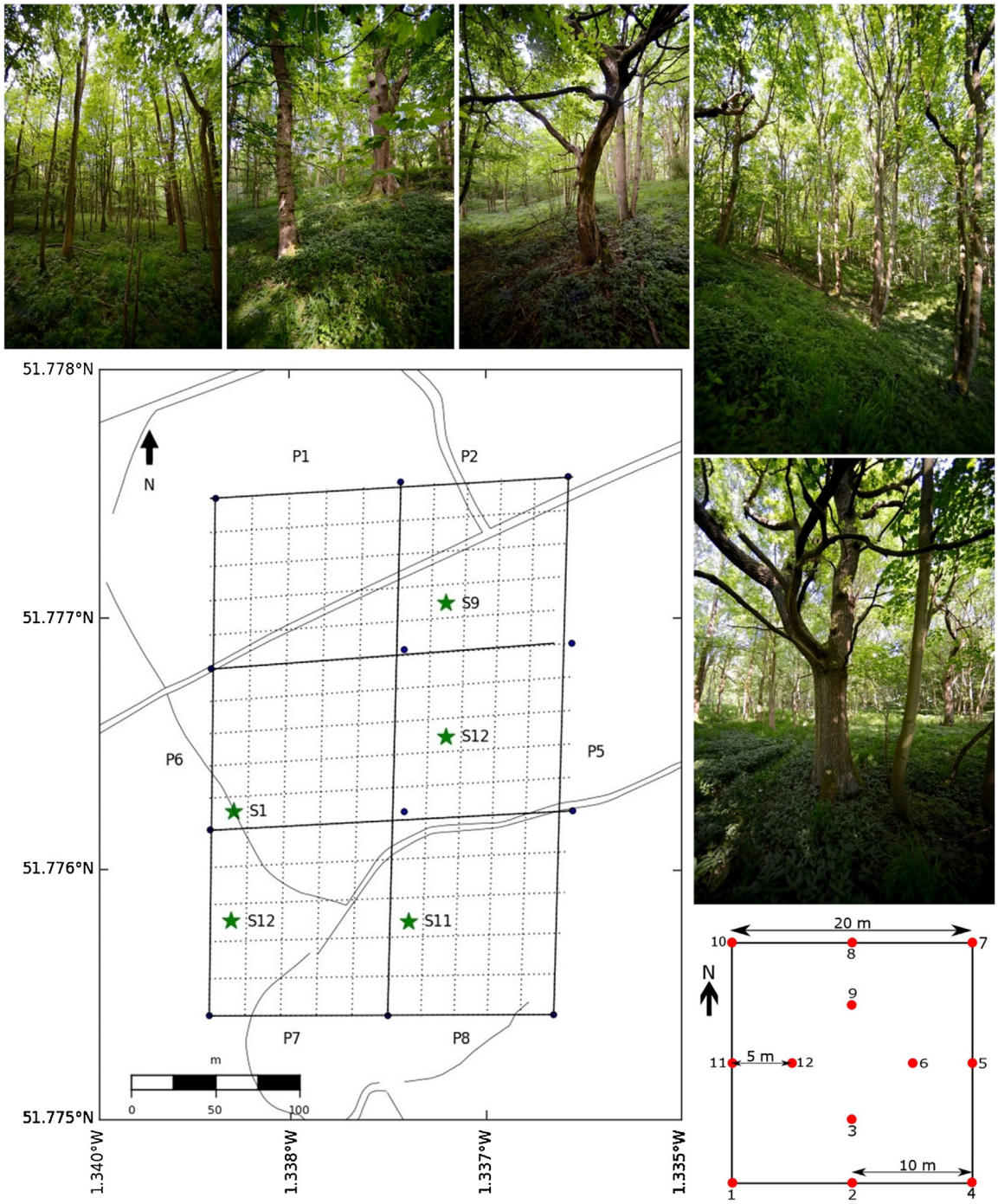

Fig. 1. Clockwise from top: P2S9; P5S12; P6S1; P7S12; P8S11; the VALERI sample design with images acquired at each location marked by a red dot; the locations of the subplots that were measured (stars) in the wider 6 ha site, the solid and dotted black lines give the plot and subplot boundaries (estimated from GPS readings). (For interpretation of the references to colour in this figure legend, the reader is referred to the web version of the article.)

coefficient of variation of the RMSE ($CV(RMSE) = \frac{RMSE}{\bar{y}}$ where $\bar{y}$ is the mean of the dependent variable), a unitless analogue of the RMSE which allows comparisons between values; the coefficient of determination adjusted for sample size (R^2_{adj}), which describes the proportion of the variance explained by the model for least squares regression; and the concordance correlation coefficient (ρ_{CCC}), which describes the degree of agreement between two variables (Lin, 1989).

2.3. User variability

A supplementary exercise was carried out in an attempt to quantify the uncertainty associated with the camera operator upon the measurement procedure. These measurements were acquired at three locations within a wooded area of a nearby London park. At each location, nine users collected hemispherical photographs after being briefed on the measurement procedure set out in

Fig. 2. User setting up a tripod levelled DHP (far left – compass positioned over camera lens) with bubble level attachment (middle left) and using the hand-levelling approach (middle and far right).

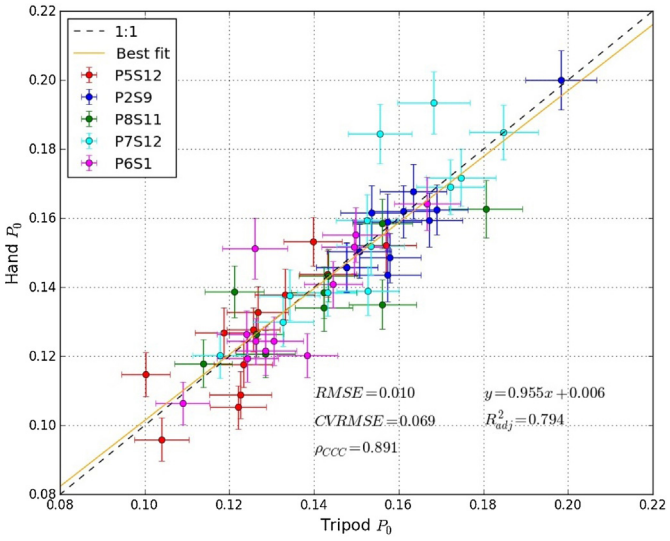

Fig. 3. Comparison of the average gap fraction per image for hand- and tripod-levelled techniques. Error bars represent the SEOM at the $k = 2$ coverage interval.

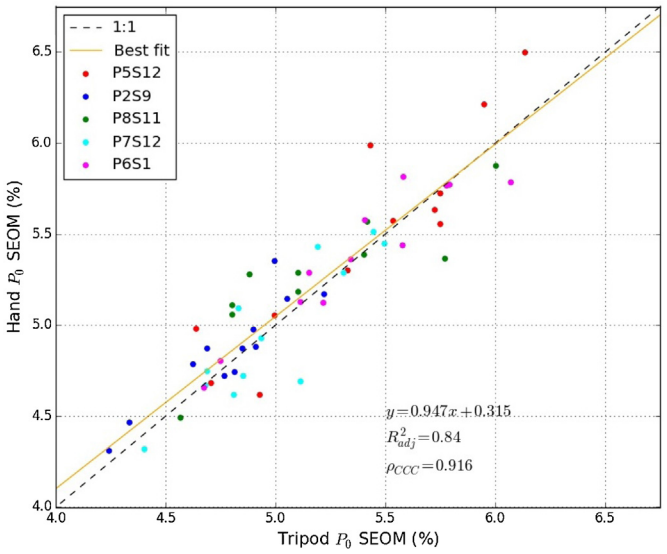

Fig. 4. Comparison of the variability of the hand- and tripod-levelled techniques as measured by the relative SEOM across each image.

Section 2.1.2. The measurements were taken in quick succession in order to minimise the effects of changing illumination conditions. The resulting images were processed using equivalent settings and the gap fraction values for each image were returned.

3. Results

All subplots were comprised of 12 image pairs with the exception of P8S11, which consisted of 10 image pairs (2 pairs were removed due to a quality issue). Due to the limited number of sample subplots, the image gap fraction statistics were used to better analyse the comparability between the tripod and hand levelling methods.

Pairwise comparison of image-averaged P_0 (i.e. from each measurement location) across all subplots (Fig. 3) displayed a 1:1 relationship with 79.4% of the variation explained by the linear agreement between tripod and hand-levelled estimates. Gap fraction occupies a range of approximately 0.1–0.2 with values from some subplots (e.g. P2S9) being clustered together while others (e.g. P7S12, P6S1 and P8S11) are more widely dispersed over this range. The average deviation from the best fit line, as reported by RMSE and CV(RMSE) values of 0.01 and 0.069, is approximately 6.9% of the average P_0.

The pairwise comparison of the standard error of the within-image P_0 mean ($\frac{\sigma_{P_0}}{\sqrt{n}}$, where n is the number of cells for which P_0 is calculated) exhibits a similar relationship to the average (Fig. 4) with 84% of the variation explained by the relationship between the two techniques. Unlike the average gap fraction, the standard error of the mean (SEOM) is more spread out over the full range of the values at the subplot level. The range of SEOMs for the image-specific gap fraction was approximately 4.3–6.5%.

Fig. 5 shows the image-specific gap fraction binned by zenith angle (10° bin range averaged across all azimuth angles) and colour coded for subplot. The sampled zenith angle range (θ) extends from 0 to 60°. The range of gap fraction values (i.e. min[P_0] – max[P_0]) contracts while the mean decreases with increasing zenith angles. In general the RMSE values decrease with increasing zenith angle while the CV(RMSE) follows a similar trend until $\theta > 50°$ where the values jump slightly (possibly due to the P_0 values decreasing further). By contrast, the R^2_{adj} and ρ_{CCC} do not show dependency with zenith angle and range between 0.75–0.89 and 0.87–0.94 respectively.

Fig. 6 shows the aggregated subplot level values of P_0 and PAI_e. Both show high R^2_{adj} values at 0.89 and 0.92 respectively while the SEOMs given for the P_0 graph indicate that the spread in values accounts for approximately 1.5% of the gap fraction value and

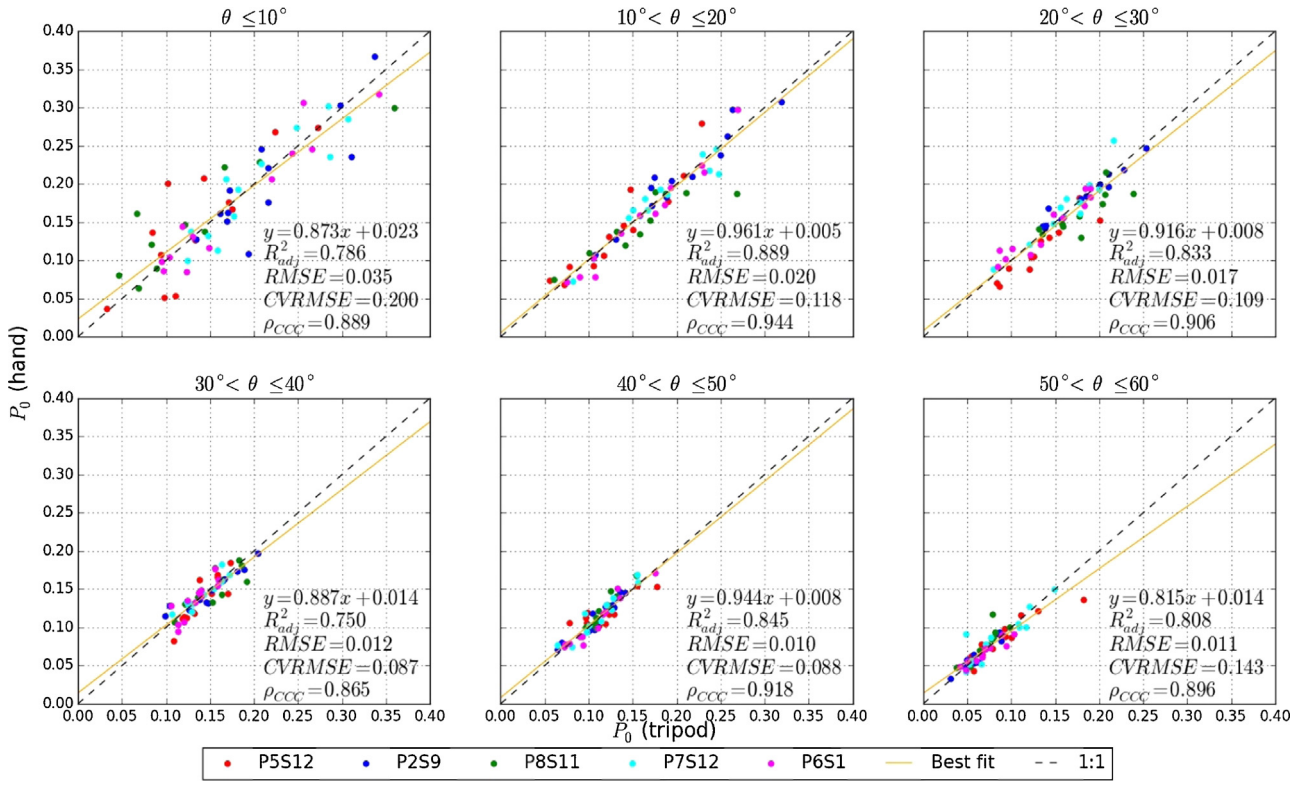

Fig. 5. Comparison of hand- and tripod-levelled gap fraction as computed by CAN-EYE for 10° zenith rings.

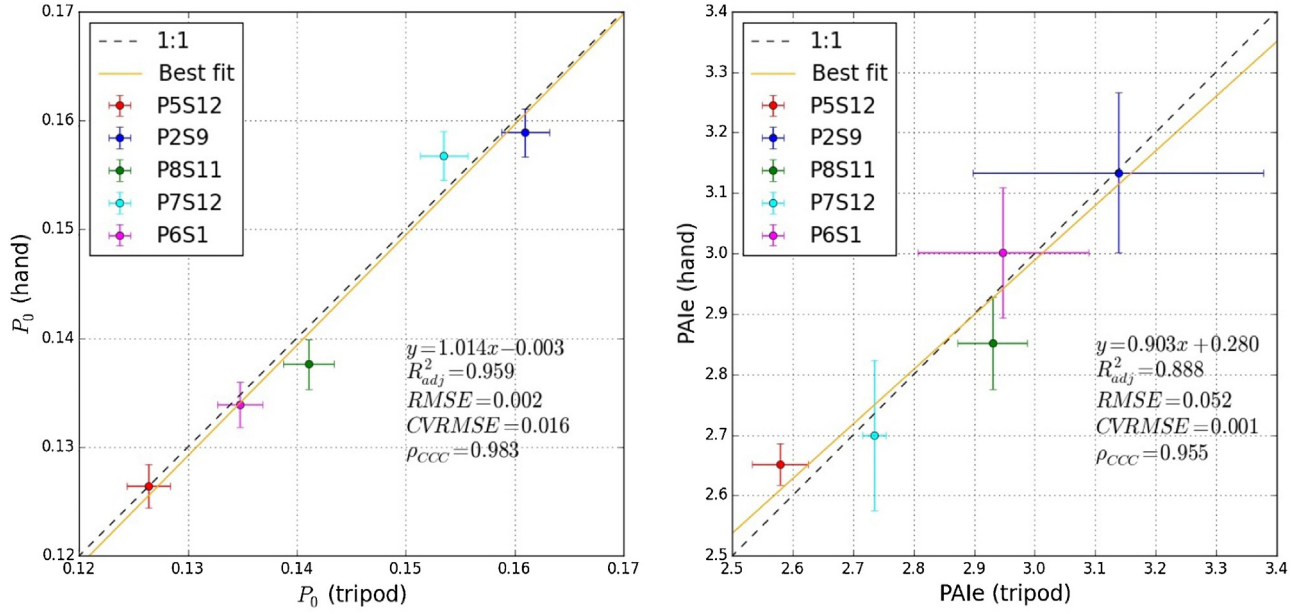

Fig. 6. Comparison of mean gap fraction (left) and PAI (right) from tripod- (*x*-axis) and hand-levelled (*y*-axis) hemispherical photography. The error bars represent the SEOM of the subplot P_0 at a coverage factor of $k = 2$ (left plot) and an uncertainty metric accounting for both the look-up table inversion and measured-to-modelled P_0 RMSE at $k = 2$ (right).

is approximately equal in both *x* and *y* directions. At the PAI_e level, an uncertainty metric accounting for the inversion error and measured-to-modelled P_0 RMSE (INRA, 2013) varies between 0.7 and 7.6%. Unlike P_0, this variation can differ in the *x* and *y* directions.

The hand-levelling technique was found to be roughly 5–8 times quicker across all subplots (with varying local terrain). We were able to complete a single subplot (that is a VALERI unit of 12 locations – discussed in Weiss et al. (2004)) in approximately two minutes using the hand-levelling approach, this compares to approximately 10–15 min (easy terrain) or 30 min (difficult terrain) for the tripod-levelled DHPs over the same area. However the exact time will depend on the nature of the subplot and the wider site, the vegetation density, topography, and user. Importantly, many of these factors will also influence the speed at which a VALERI plot using tripod-levelling can be completed. Our observation, at this site and over a range of local terrains, is that the majority of time

taken during the hand-levelled approach was walking between photograph locations, while the majority of time spent during the tripod-levelled approach was spent levelling the camera.

In the supplementary exercise (Section 2.3) examining the user variability associated with hand levelling the total variability for each location was approximately 5% (1σ with $\mu = 5.41\%$). Under the assumption that the variability follows a Gaussian distribution and that it is consistently around 5%, the impact of the variability decreases by $1/\sqrt{n}$ with the number of samples (n) acquired. In this case, with 12 samples per subplot, this estimated user uncertainty drops to 1.56% (1σ). These are suggested as indicative 'worst case' values since the consistency is likely to improve with practice, while it is expected that researchers acquiring multiple hemispherical photographs will also have a vested interest in the data quality.

4. Discussion

This study tested the common recommendation that tripod-levelling is required when producing hemispherical photographs for determination of P_0 and PAI_e in forest canopies (Chianucci and Cutini, 2012; AusCover, 2015; TERN, 2015; Woodgate et al., 2015). This was assessed using image-to-image comparisons of tripod- and hand-levelled techniques for estimating P_0 as well as VALERI subplot comparisons for P_0 and PAI_e averaged over all images in a subplot.

At the image-level, P_0 displays a 1:1 relationship (Fig. 3) when both techniques are compared with an R^2_{adj} of 0.794, while the best-fit residuals do not depend on the gap fraction within the range of the observations. The reduced sensitivity in the hand-levelled values when compared with the tripod-levelled values is most likely to arise from the limited range of gap fraction values that are present in the study area. It is our expectation that incorporation of a wider range of P_0 values (e.g. from sites with denser or sparser canopy cover) would see the slope parameter tend to one and the offset to zero. A similar relationship is seen when the relative image P_0 SEOM values are compared (Fig. 4). This suggests that over the whole image (i.e. the smallest unit from which PAI_e is calculated) the relationship between the two techniques is stable.

Fig. 5 shows the comparison of the two techniques with respect to zenith angle. As expected, the 10° surrounding the zenith display the largest range of values as well as the greatest degree of spread, as highlighted by the RMSE and CV(RMSE). As the zenith angle increases the general trend is one of reducing range of P_0 as well as a general reduction in the magnitude. This is to be expected as each pixel corresponds to a longer canopy path length with increasing zenith angle from the image centre. Consequently, gaps are less likely as the path length through the canopy increases.

Effectively this means that the importance of the levelling procedure is inversely proportional to the zenith angle. Consequently, at 57.5° where PAI_e is independent of leaf angle and where formulations for the retrieval of PAI_e exist (Warren-Wilson, 1963; Bonhomme et al., 1974), the impact of the levelling procedure should be small. In fact, for PAI_e estimated from P_0 over the whole image (Fig. 6) using the model-based inversion technique implemented in CAN-EYE (V6.1, INRA (2013)), the best fit errors, as given by the CV(RMSE), account for < 1%. This, coupled with a $\rho_{CCC} = 0.955$, provides a good indication of the comparability of the two techniques given the absence of an independent reference. Furthermore, the error bars in Fig. 6 illustrate that the majority of the mismatch between the two techniques falls within the variability of the gap fraction and PAI_e retrieval error. Even so, the image- and subplot-level P_0 SEOMs are equal for both techniques indicating that neither technique can provide more precise P_0 estimates.

The results show that these techniques produce comparable estimates of gap fraction and PAI_e under equivalent conditions. However, in terms of implementation, hand-levelling is superior due to the reduced time required to complete a measurement. It was noted that under the conditions present for this study this could be up to 8 times faster than the tripod-levelled measurements. The time saved using the hand-levelled approach can be better utilised by sampling a larger area or obtaining a greater number of samples and thus increasing the precision of the PAI/PAI_e estimates or reducing the total time required in the field. Likewise, the speed of data acquisition allows measurements during short-lived illumination conditions. Other advantages are logistical: less equipment to carry to the field site, less training required to conduct measurements and easier data acquisition in difficult terrain.

5. Conclusion

Many authors advise the use of a tripod-levelling procedure for accurate determination of plant/leaf area index from DHP (Chianucci and Cutini, 2012; AusCover, 2015; TERN, 2015; Woodgate et al., 2015). The results presented here show that P_0 and PAI_e derived from DHPs acquired with hand-levelling can differ by < 2% from tripod-levelled DHPs under equivalent conditions. To our knowledge, this is the first quantitative test of this aspect of DHP acquisition in the field.

The significance of these results is increased when the potential time savings that can be made by utilising the hand-levelling technique are considered.

We suggest that in situ LAI/PAI sampling protocols are updated with the recommendation that the decision between tripod- and hand-levelling is left up to the practitioner, while acknowledging that hand-levelled DHPs deliver marginal differences (< 2% on average in this case) when compared to tripod-levelled DHPs, but in a fraction of the time.

Acknowledgments

The authors would like to thank Nigel Fisher and Yadvinder Malhi for their support and for allowing us to use Wytham Woods for this study; Marie Weiss for her support with CAN-EYE; the anonymous reviewers for their comments; and colleagues at NPL for assisting in the user variability experiment. The research leading to these results was partially funded through the Metrology for Earth Observation and Climate project (MetEOC-2), grant number ENV55 within the European Metrology Research Programme (EMRP). The EMRP is jointly funded by the EMRP participating countries within EURAMET and the European Union. This work was also supported by the UK government's Department for Business, Energy and Industrial Strategy. M. Disney acknowledges partial support for this work via NERC NCEO, EU Seventh Framework Programme (FP7/2007-2013) project QA4ECV under grant agreement no. 60740, and the NERC GREENHOUSE project (NE/K00254/1).

References

AusCover, 2015. Hemispheric Photography Protocol. http://www.auscover.org.au/xwiki/bin/view/Field+Sites/Hemispheric_Protocol (accessed 09.02.16).

Baret, F., Weiss, M., Garrigues, S., Leroy, M., Jeanjean, H., Fernandes, R., Myneni, R., Privette, J., Morisette, J., Bohbot, H., Bosseno, R., Dedieu, G., Di Bella, C., Duchemin, B., España, M., Gond, V., Gu, X-F., Guyon, D., Lelong, C., Maisongrande, P., Mougin, E., Nilson, T., Veroustraete, F., Vintilla, R., 2003. VALERI: A Network of Sites and A Methodology for the Validation of Medium Spatial Resolution Land Satellite Products. http://w3.avignon.inra.fr/valeri/documents/VALERI-RSESubmitted.pdf (accessed 09.02.16).

Bonhomme, R., Varlet-Grancher, C., Chartier, P., 1974. The use of hemispherical photographs for determining the leaf area index of young crops. Photosynthetica 8, 299–301.

Butt, N., Campbell, G., Malhi, Y., Morecroft, M., Fenn, K., Thomas, M., 2009. Initial results from establishment of a long-term broadleaf monitoring plot at Wytham Woods, Oxford, UK. Technical Report. University of Oxford.

Chen, J.M., Black, T.A., 1992. Defining leaf area index for non-flat leaves. Plant Cell Environ. 15, 421–429.
Chianucci, F., Cutini, A., 2012. Digital hemispherical photography for estimating forest canopy properties: current controversies and opportunities. iForest 5, 290–295.
España, M., Baret, F., Weiss, M., 2008. Slope correction for LAI estimation from gap fraction measurements. Agric. For. Meteorol. 148, 1553–1562.
Fernandes, R., Plummer, S., Nightingale, J., Baret, F., Camacho, F., Fang, H., Garrigues, S., Gobron, N., Lang, M., Lacaze, R., Leblanc, S., Meroni, M., Martinez, B., Nilson, T., Pinty, B., Pisek, J., Sonnentag, O., Verger, A., Welles, J., Weiss, M., Widlowski, J.L., Schaepman-Strub, G., Roman, M., Nickeson, J., 2014. Global Leaf Area Index Product Validation Good Practices. Committee on Earth Observation Satellites, Working Group on Calibration and Validation, Land Product Validation Sub-Group. 2. 0 edition.
Glatthorn, J., Beckschäfer, P., 2014. Standardizing the protocol for hemispherical photographs: accuracy assessment of binarization algorithms. PLOS ONE 9, e111924.
INRA, 2013. CAN EYE. INRA, Avignon, France, v 6.3.13 edition. Available from: http://www6.paca.inra.fr/can-eye/Documentation-Publications/Documentation (accessed 10.09.15).
Leblanc, S.G., Chen, J.M., Fernandes, R., Deering, D.W., Conley, A., 2005. Methodology comparison for canopy structure parameters extraction from digital hemispherical photography in boreal forests. Agric. For. Meteorol. 129, 187–207.
Lin, L.I.K., 1989. A concordance correlation coefficient to evaluate reproducibility. Biometrics 45, 255–268.
Macfarlane, C., Ryu, Y., Ogden, G.N., Sonnentag, O., 2014. Digital canopy photography: exposed and in the raw. Agric. For. Meteorol. 197, 244–253.
Morisette, J.T., Baret, F., Privette, J.L., Myneni, R.B., Nickeson, J.E., Garrigues, S., Shabanov, N.V., Weiss, M., Fernandes, R.A., Leblanc, S.G., Kalacska, M., Sánchez-Azofeifa, G.A., Chubey, M., Rivard, B., Stenberg, P., Rautiainen, M., Voipio, P., Manninen, T., Pilant, A.N., Lewis, T.E., Iiames, J.S., Colombo, R., Meroni, M., Busetto, L., Cohen, W.B., Turner, D.P., Warner, E.D., Petersen, G.W., Seufert, G., Cook, R., 2006. Validation of global moderate-resolution LAI products: a framework proposed within the CEOS land product validation subgroup. IEEE Trans. Geosci. Rem. Sens. 44, 1804–1814.
Promis, A., Gärtner, S., Butler-Manning, D., Durán-Rangel, C., Reif, A., Cruz, G., Hernández, L., 2011. Comparison of four different programs for the analysis of hemispherical photographs using parameters of canopy structure and solar radiation transmittance. Waldokol. Online 11, 19–33.
Pueschel, P., Buddenbaum, H., Hill, J., 2012. An efficient approach to standardizing the processing of hemispherical images for the estimation of forest structural attributes. Agric. For. Meteorol. 160, 1–13.
Schaefer, M.T., Farmer, E., Soto-Berelov, M., Woodgate, W., Jones, S., 2014. Overview of ground based techniques for estimating lai. In: Soto-Berelov, M., Held, A., Phinn, S., Jones, S. (Eds.), AusCover Good Practice Guidelines: A technical handbook supporting calibration and validation activities of remotely sensed data products. TERN AusCover, pp. 90–122.
Sea, W.B., Choler, P., Beringer, J., Weinmann, R.A., Hutley, L.B., Leuning, R., 2011. Documenting improvement in leaf area index estimates from MODIS using hemispherical photos for Australian savannas. Agric. For. Meteorol. 151, 1453–1461.
STRI, 2008. Smithsonian tropical research institute. http://www.ctfs.si.edu/plots/summary/ (accessed 03.06.16).
TERN, 2015. SuperSites vegetation monitoring protocols. In: Karan, M. (Ed.), TERN, Australian SuperSite Network. 1.21 edition. , Available from: http://www.supersites.net.au/images/resource/SuperSites_Vegetation_Monitoring_Protocols_Ver1.21.pdf (accessed 14.06.16).
Warren-Wilson, J., 1963. Estimation of foliage denseness and foliage angle by inclined point quadrats. Aust. J. Bot. 11, 95–105.
Weiss, M., Baret, F., Smith, G., Jonckheere, I., Coppin, P., 2004. Review of methods for in situ leaf area index (LAI) determination – Part II. Estimation of LAI, errors and sampling. Agric. For. Meteorol. 121, 37–53.
Woodgate, W., Armston, J.D., Disney, M., Jones, S.D., Suarez, L., Hill, M.J., Wilkes, P., Soto-Berelov, M., 2016. Quantifying the impact of woody material on leaf area index estimation from hemispherical photography using 3D canopy simulations. Agric. For. Meteorol. 226–227, 1–12.
Woodgate, W., Jones, S.D., Suarez, L., Hill, M.J., Armston, J.D., Wilkes, P., Soto-Berelov, M., Haywood, A., Mellor, A., 2015. Understanding the variability in ground-based methods for retrieving canopy openness, gap fraction, and leaf area index in diverse forest systems. Agric. For. Meteorol. 205, 83–95.